ASHESI UNIVERSITY

ISLANDING DETECTION AND CONTROL IN DISTRIBUTED GENERATIONS

BSc. ELECTRICAL AND ELECTRONIC ENGINEERING

BENJAMIN GOMADO

2021

ASHESI UNIVERSITY

ISLANDING DETECTION AND CONTROL IN DISTRIBUTED GENERATIONS

CAPSTONE PROJECT

Capstone Project submitted to the Department of Engineering, Ashesi University in partial fulfilment of the requirements for the award of Bachelor of Science degree in Electrical and Electronics Engineering.

BENJAMIN GOMADO

2021

DECLARATION

I hereby declare that this capstone is the result of my own original work and that no part of it has been presented for another degree in this university or elsewhere.

Candidate's Signature:

……

Candidate's Name:

……

Date: ……

I hereby declare that preparation and presentation of this capstone were supervised in accordance with the guidelines on supervision of capstone laid down by Ashesi University.

Supervisor's Signature:

……

Supervisor's Name:

……

Date: ……

Acknowledgements

My first and foremost sincere thanks go to the Lord God Almighty for his grace, mercies, and goodness bestowed on me throughout my entire life at Ashesi University. The Lord has always been with me, and His faithfulness is forever. His love abounds, his countenance is always present, his grace is always sufficient, and ultimately, his provisions are always timely. This project would not have been successful if it had not been him who granted me strength good health.

A very special thanks go to Mr. Akparibo Richard Awingot, my indefatigable supervisor. It is undeniable fact that this project would not have become a reality if it had not been for his supports and encouragement. In the face of tough times, and when I was at the verge of giving up, his encouragement become stronger, and he stood with me throughout the project. I would like to thank Dr. Amanquah Nathan, the Dean of Engineering. He has been a father to me throughout my studies and in this project as well. His timely guidance and numerous advice offered to me need to be appreciated.

Also, not forgetting Mr.Tali Nicholas for his timely provision of components and advice. He made sure that the working tools required were made available in time, and that is well appreciated. I would also like to register my appreciation to all my able lecturers, especially those who taught me from freshman year to my final year. It is their pieces of knowledge impacted me that have culminated in the actualization of this great project. Also, a big thanks to all my colleagues and other friends whose advice and encouragement aided me to undertake this project. May the Lord bless you all and keep you.

Abstract

Despite the numerous environmental and economic benefits of the integration of renewable distributed generation (DG) into the distribution network of power systems, there are a number of technical challenges that come with it. Unintentional islanding is one of the critical issues regarding DGs integration into the distribution grid. Unintentional islanding occurs when DG suddenly becomes electrically isolated from the main grid but continues to energize the local loads it serves or portion of the power system. In the event of unintentional islanding, frequency voltage and the rest of parameters for power system may be completely out of the acceptable limits, as the island formation is unregulated. The unintentional islanding is undesirable in power system as it can severely damage loads, risk the life of utility line workers. It is, therefore, imperative to develop an islanding controls strategy that helps mitigate the unintentional islanding phenomenon in DGs.

In this project work, Rate of change of voltage (ROCOV), Change in sine waveform at the output of inverter during islanding and, total harmonic distortion of voltage $\mathrm{THD}(_{\mathrm{V}})$, are the islanding detection methods designed and employed for detecting unintentional islanding. A 100-kW photovoltaic system was designed and modelled as the DG for the study, and hence the project considers only inverter-based DG. MATLAB Simulation was then carried out for the detection and control of unintentional islanding. After several iterations of the simulation, the desired results from the simulation were obtained. Based on the results from the project, certain recommendations were made, and the project design can be implemented on a live DG system.

Table of Contents

Contents **Page**

Chapter 1: General Introduction

1.1 Background

As the world advance in technology and increases in human population, there is a demand for high electricity across the globe. Electricity is the backbone of every country as it is essential, and without it, industries cannot run. The increase in the demand for clean and reliable energy resources calls for high penetrations of DGs into the conventional grid. Technological advancements such as gas turbines, wind turbines, micro-hydro, photovoltaic, and the current innovation in power electronics, deregulation of the electricity market are the drivers for DGs. Also, customers' demand for better power reliability and quality, and more importantly, the concern for the environment regarding decarbonization, are causing a shift in the power industry towards DGs [1].

Distributed generations are power generation resources that are close to the load they serve, and they are normally located at the customer site, unlike the conventional production of energy, which are centralized [1]. The integration of Distributed Generations into the traditional grid reduces transmission losses as they are normally situated close to the load they serve and do not require long transmission lines [1]. The Electric Power Research Institute (EPRI) defines a DG as a small generation (1kW to 50MW) or energy storage system which are built near customer loads and to sub-transmission or distribution station [2]. The level of DG penetration in a distribution system is increasing because DGs can save the cost of transmission and distribution (T&D) capacity upgrades, minimize distribution and transmission line losses, improve voltage profile, improve power quality of the system [3]

From the foregoing definitions of DGs, it can be seen that DGs have some advantages over the centralized generations. However, DG interconnection into the electricity network causes some protection menaces such as safety, islanding, and short-circuit currents [4]. Islanding condition

comes in two basic types: unintentional and intentional islanding. Unintentional islanding happens when a portion of the distribution network becomes inadvertently and electrically isolated from the utility grid, and the rest of the power system yet continues to be energized by the DG connection to the isolated subsystem [5]. Normally, intentional islanding occurs when a portion of the distribution network is deliberately isolated from the main utility grid for maintenance purposes. This is done such that there is a minimal mismatch between generation and load [6].

This project focuses on unintentional islanding detection and control. Rate of change of voltage (ROCOV) and change in sine waveform at the output of the inverter are the two main detection methods employed in this research. The control is achieved by opening both upstream (grid side) and downstream (DG side) circuit breakers when voltage is below a certain threshold value. Also, when the sine waveform at the output of the inverter is distorted and does not follow the normal grid AC shape. In doing this, $100kW$ Solar power plant would be designed and model in MATLAB as a case study. The project is organized into six chapters: Introduction, Literature Review, Design Methodology, Results and Discussions, and Conclusions and Recommendations, respectively.

1.2 Problem Definition

Islanding is a condition in which a distribution network becomes electrically isolated from the rest of the power system but continues to be energized by DG connected to it. With a traditional distribution network, it does not have any active power generating source in it, and it does not get power in case of a fault in the transmission line upstream, but this is not the case with DG. This is because DGs power local loads, and in the event of islanding where the DG is disconnected from the national grid, the DG source still continue to serve the loads.

Utility worker's safety can be compromised by DG sources connecting a network after primary sources have been opened and tagged out. This is a threat to the line workers whenever the main grid is down, and they need to work on it.

Also, whenever islanding occurs, there is an irregular reclosing, which could result in out-of-phase reclosing of DG. This, in effect, causes large current and mechanical torques to be created, and eventually, prime movers and generators can be damaged [6]. Again, the instantaneous reclosing creates transient, which has the potential of damaging utility and loads at the consumer end [7].

In the event of islanding, frequency and voltage are out of the standard permissible level. This can affect the power quality of the power system. In addition, whenever islanding occurs, there is a possibility that the islanded system may not be grounded by the DG interconnection, and without the proper grounding, the power system becomes highly unstable.

In other to safeguard the power system in the event of islanding conditions, the IEEE 929-1988 standard demands DG disconnection when it is islanded [8]. And the utilities require the DG disconnection from the national grid as fast as possible, as this is the current practice [8]. The IEEE 1547-2003 standard [9] also states that in the event of unintentional islanding, all DG must take a maximum of 2 seconds for detection and ceases to continue energizing the distribution network.

1.3 Objective of the Project Work

The specific objectives of this project would include:

1. Design and model a DG of a 100kW photovoltaic grid-connected network.
2. Design and model a passive islanding detection method that detects unintentional islanding in inverter based DGs and be able to differentiate non-islanding events.

3. Improve upon the islanding detection time and save cost.
4. Demonstrate practical implementation of passive islanding detection method by way of Simulink model simulation.

1.4 Motivation of Project Work

Looking at the electricity grid in Ghana currently, there has not been much penetration of DGs into the National Grid. However, the government of Ghana has a plan to ensure that there is 10% renewable energy integration into the national grid by the end of 2022 [10]. In the quest for Ghana to meet this target by 2022, some renewable energy plants have been completed, and some are underway to be completed and commission. Currently, Ghana has a Navrongo solar power plant of 2.5MW and a mini-hydro of 45kW, which are operational, and grid-connected [10]. A 225MW Ayitepa wind power plant is awaiting government approval and is expected to start soon [10]. Nzema solar station of 20MW is seeking an Energy Performance Certificate, Kaleo and Lawra solar power plant of a total installed capacity of 17MW is currently under construction and expected to be completed and grid-connected by ending of 2021 [10]. There are other Independent Power Producers (IPP) like BXC of 20MW, and so on.

From the above considerations, it can be seen that the conventional grid is receiving some amount of DGs penetration. This consideration suggests that the National Grid in Ghana would have received substantial DGs integration in some few years to come. For a successful DG integration, unintentional islanding must be detected on time with a robust and practical islanding detection method. Therefore, one of the motivations for this project is the need for an effective islanding detection method that detects unintentional islanding effects in DGs on time. Another motivation for this project is the current technological advancement in smart grid systems and the rising need for a sustainable environment in terms of low carbon footprint.

1.5 Research Methodology

The scientific methods of research are followed and used to arrive at the research goals. The research methods include.

1. Defining and redefining the objective of the projects.
2. Systematic literature Review
3. Computer Design and modelling.
4. Computer Simulation of Design modelling

1.6 Research Facilities Used

The research facilities used for this project work include:

1. Computer, internet, and Library facilities at Ashesi University
2. Electrical and Electronics Laboratory at Ashesi University
3. Mechanical workshop at Ashesi University

1.7 Scope of work

The project mainly focuses on unintentional islanding detection and control in Distributed generations. A 100kW photovoltaic grid-connected system is systematically design and model in MATLAB as the DG understudy for this project. The ROCOV , Output waveform of the inverter and THD passive islanding detection methods are used and are evaluated on their practical implementation, cost and detection time. The scope does not include active islanding detection methods and multiple DGs systems.

1.8 Project Organization

The subsequent pages include the chapters of literature review on various islanding detection methods and controls, a design of islanding model by the use of simulation software, the islanding algorithm method used in the project, the implementation of the algorithm, result and analysis, recommendation, and future works.

Chapter 2: Literature Review

2.1 Introduction

In this chapter, islanding in Distributed Generations is discussed. The various types of islanding and how they occur are vividly explained with clear examples. The chapter furthers the discussion on the various islanding detection algorithms such as passive method, active method, and communication method with their pros and cons. The chapter finally delved into the review of related works about the focus of this project.

2.2 Islanding in Distributed Generations

The integration of Distributed Generations into the utility network comes with many benefits. Among these benefits are peak shaving, increase overall energy efficiency, reductions in line losses, environmental impact reductions, relieved transmission and distribution congestions, and many more.

Electrical islanding is a situation in a power system where part of the electrical network is disconnected from the main utility grid due to an open circuit. The cause of the open circuit may be due to opening of an upstream circuit breaker, fuses blowing, conductors physically breaking, and so on. The common cause of islanding in power system is opening of an upstream circuit breaker. Electrical islanding is of two types, thus intentional islanding, and unintentional islanding. Intentional islanding occurs when the downstream circuit breaker is open such that the DG can dedicatedly power the local loads it serves. This is done when the power quality in the main grid is poor such that it can affect the loads. Also, intentional islanding can occur in a power system in the event of routine maintenance where the DG, including the load, is isolated from the main grid at the point of minimal mismatch of frequency and Voltage.

For unintentional islanding, the upstream circuit breaker opens suddenly due to malfunction. In the event of this unintentional islanding, the DG continues to excite the feeder network and its local loads. This is undesirable as it has the tendency to compromise the safety of the utility line workers, damage electrical loads and DGs due to out of reclosing of the reclosers and transients in voltage and frequency that accompany them.

For a sustained island in power system, it is required to have a stable operating point for DG with the load. Also, it is required that the real and reactive power match between DG and load.

2.3 Islanding Detection Standards

There are several internationally accepted standards that have been stipulated by organizations like IEEE and IEC for interconnection, operation, and control of DG power systems with the main utility grid. The standards stated certain requirements that are imperative to the testing, safety considerations, performance, and maintenance of DG integration into the distribution power system networks. IEEE 1547 and UL-1741 are standards for anti-islanding protection used in the evaluation of the performance for the various Islanding Detection Methods [11]. The main items in the islanding detection standard documents include: DG unit must be able to disconnect within 2s time limit, in an event where the main utility grid is out of service. There should be proper control for frequency, voltage, and power quality. Non-contributing and the contributing DG should be appropriately identified. Adequate monitoring of the magnitude and direction of the power flow. And the functionality and characteristics of the DG units should be well observed. These standards aid researchers in the designing of robust and efficient IdMs. The table below stated the various standard for islanding detection in a power distribution network.

Table 2.1: Standards for Islanding Detection [7]

Parameters	IEEE Std. 1547-2003	EEE Std.929-2000	IEC 62116	Korean Standard
Quality Factor	1	25	1	1
Detection Time	t < 2s	t < 2s	t < 2s	t < 0.5s
Allowed Frequency Range(nominal frequency f_o)	59.3 Hz $\leq f \leq$ 60.5 Hz	59.3 Hz $\leq f \leq$ 60.5 Hz	(f_o -1.5 Hz $\leq f$ and $f \leq$ (f_o +1.5 Hz)	59.3 Hz $\leq f \leq$ 60.5 Hz
Allowed Voltage Range (nominal Voltage V_o)	0.88 $\leq V \leq$ 1.10	0.88 $\leq V \leq$ 1.10	0.85 $\leq V \leq$ 1.15	0.88 $\leq V \leq$ 1.10

2.4 Islanding Detection Methods

Different islanding detection methods have been developed over the years. Li et al. provided a detailed review on islanding detection in their work [12]. The paper reviewed the various Islanding Detection Methods (IDM). The IDM could be broadly classified into remote and local methods depending on their location in the DG power system [13]. While the remote methods are anti-islanding algorithms at the grid side, the local is based on the DG side. The local method was also classified into passive and active methods. The basic idea of the local method was on the measurement of variables at the side of the microgrid or DG. Passive methods detect islanding by monitoring parameters such as voltage, current, frequency, and phase. Active methods send or inject disturbance intentionally to detect if the disturbance affects the frequency, voltage,

impedance parameters, or power. Remote methods seek to monitor the status of circuit breakers immediately islanding conditions occur, and this is based on communication between the main utility grid and the DGs. The remote method is characterized by a very small or no non-detection zone (NDZ), and it is an important characteristic as it does not affect or impact the power quality. Remote methods are commonly used in multiple-inverter power systems because they are very effective. However, they need a larger amount of investment for implementation. It is also not economical in a single-inverter power system. The various methods for detecting islanding in DGs have their own strength and weaknesses. The subsection further discusses the various methods under the remote and the local anti-islanding algorithm.

2.4.1 Passive Methods

Passive methods of islanding detection generally monitor the changes of power quality parameters such as voltage, frequency, phase shifts before and after islanding phenomenon at the output of the DG [14]. When DG is in normal grid connections, these power quality parameters are within acceptable or desire limits. After an unintentional islanding event, the voltage, frequency and phase, and other power quality factors are out of the threshold or standard limits. The passive method detects the presence of islanding conditions by using voltage and current harmonics detection, over/under voltage, and over/under frequency (OV/UF), rate of change of frequency (ROCOF), rate of change of power output, phase jump detection, voltage unbalance [15]. The drawback of ROCOF is that it requires a minimum power mismatch of 15%, and its performance can be affected by the type of loads and the generator inertia constant [14]. The current and harmonic detection (HD) approach measures the total harmonic distortion (THD) at the point of common coupling in order to detect islanding conditions when THD is above the threshold value. This method is able to detect islanding conditions based on the principle that, during islanding

events, the inverter generates a current harmonic as a result of the distortion in the standard sine wave [16]. The distorted sin wave is transmitted to the load, and transformer hysteresis effect further increases harmonic distortion at the PCC [17]. This method is easy to implement, and its effectiveness does not change when used in multiple DGs that are connected in parallel to the same PCC. Over/under voltage and over/under frequency (OUV/OUF) is another anti-islanding method for passive islanding detection. This method is about setting a range of frequency and voltage limits. When the frequency or the voltage at the PCC is more than the threshold value, the inverters disconnect to stop supplying the load with power, and islanding is detected based on frequency and voltage deviation.

2.4.2 Active Method

For active islanding detection, there is constant communication between the distributed generator and the grid to ensure the status of the electric supply. Also, the methods are about injecting a small disturbance signal into the DG's output. By injecting the external signal, there is a significant variation in the DG parameters in the event of islanding conditions, and relays are triggered to operate. The drawback of this method is that the external signal injections can degrade the system performance as a result of harmonic disturbance and power quality problems [18]. Sliding mode frequency (SMFS), Sandia voltage shift (SVS), Sandia frequency shift (SFS), active frequency drift(AFD), and an impedance measurement(IM) are some of the examples of active IDMs [19]. The basic reason for developing active IDMs is to reduce or overcome the limitations of passive techniques, even though there are some disadvantages that come with active islanding detections.

2.4.3 Communication Method

The communication method of detecting islanding is about getting information on the status of the upstream circuit breakers and other devices. This method seeks to achieve active coordination between multiples entities in the DGs. The method can be classified into three groups, which are; Supervisory-control and data acquisition (SCADA) based methods, the use of power line communication (PLC) as a carrier for communications methods, and transfer trip methods that monitor and used to connect/disconnect from the utility grid [20]. The implementation of this method is cost-intensive as it demands communication infrastructures between the Distribution grid and the DG.

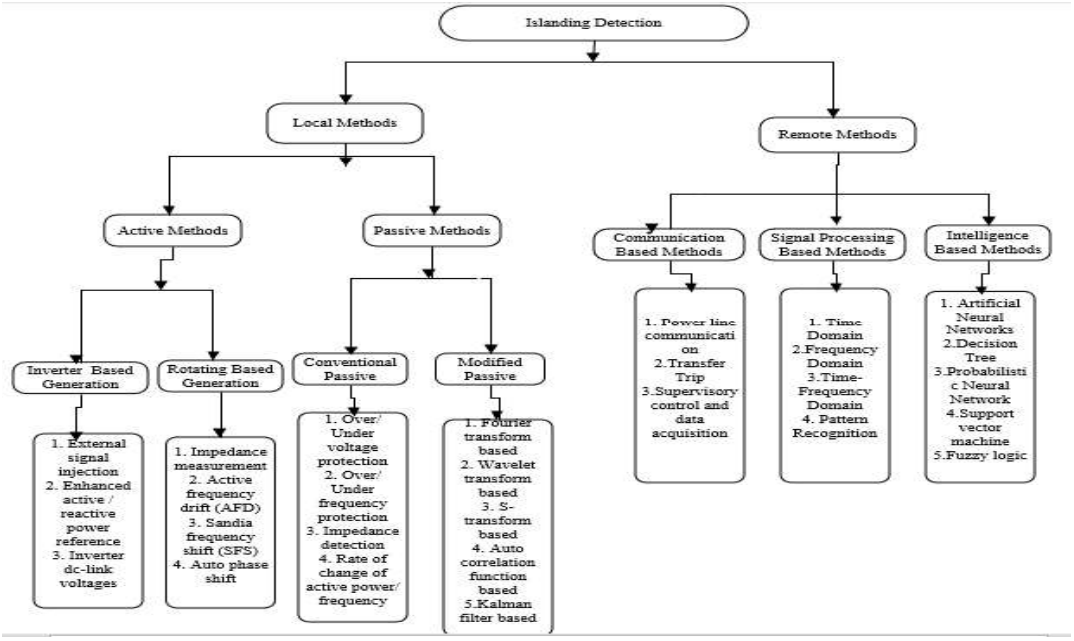

Fig.2.1: Classification of Various Islanding Detection Methods

2.4 Review of Related Work

A synchronization and intelligent load shedding algorithm for grid connection has been proposed in [21]. The paper discussed a control mechanism that was used to implement both intentional islanding and grid-connected operations of DG in microgrid. The controller supplies a constant current output during grid operation mode. The frequency and reference angle at the point of common coupling (PCC), which are important parameters for grid synchronization, were determined using phase-locked loop (PLL) control.

For current control mode, the output of the current from a designed LCL filter is converted into a synchronous frame with the help of Park's transformation and control in dc quantity so that it can be fed back and compared with the reference current. A current is then generated and sent to PI controller (current regulator) in order to generate the necessary voltage reference for the inverter.

The load shedding intelligent control is able to disconnect the system load base on priority orders and prevent the power system from any potential dangers. For the intentional islanding mode of operation, current references are generated by the controller using voltage compensators to regulate current. The load voltages are able to track their references by using a PI voltage regulator. The output of the reference currents from the compensator is compared with the load current, and the PI controller is fed by the error (differences between).

Laaksonen et al. worked on voltage and frequency control inverter-based weak LV network microgrid in [16]. The voltage and the frequency control studied were done in two cases: unintentional with unbalance power and intentional with balance power. Single Master Operation and Multi-Master Operation were two main control methods found to be possible during islanding of microgrids. The Single Master Operation is used when there is a loss of the main power supply

to the DGs, and other inverters have to work in a traditional PQ mode. In this mode of operation, a Voltage Source Inverter (VSI) is used as a voltage reference. For the Multi-Master Operation, multiple inverters work as VSI. The presence of a battery inverter with a fast response rate and operated as a single master seeks to control frequency and voltage of DGs when islanding occurs. The other inverters are connected to the grid with PQ control algorithm such that they keep the PQ in balance.

The paper concluded that including a master unit of an inverter into the microgrid helps maintain and balance frequency between the DG and the load in an islanding mode. The master unit should be interfaced with input for PLL and operated at 50Hz and also generate a 3-phase reference sine wave, which enhances the synchronism of the microgrid. The drawback of this control strategy is that both the frequency and the voltage control become heavily dependent on a master unit in an islanded mode of the microgrid.

Also, in this paper [17], a novel approach was adopted to control the voltage and frequency of microgrids in islanding operations. Inverter control based on P-Q mode and inverter control based on voltage control mode were the two control methods used in the paper. For the inverter based on P-Q mode method, there is predefined threshold points that control the reactive and the supplier's active output powers. The input power receives by the inverter is being injected into the grid, and the reactive power injected by the inverter is either set via a microgrid control center or locally. With current control techniques, the P-Q control can be realized. The phase and amplitude of the inverter are controlled in a way that the desired reactive and active powers can be achieved [22]. The Inverter Control Based on Voltage and Control Mode is operated such that with the frequency and the voltage reference values, the inverter is able to feed the loads by using a certain control

method. IEEE modified 13-bus network was used for the study, and it was realized that the islanded network comprises generation sources and loads. While one of the sources is taken as a frequency and voltage controller, the other source generates reactive and active powers defined in a range by the control center. With the help of two PI controllers, the proposed controller was required to maintain the reference bus voltage as well as the frequency of the entire network. By applying the reference values V_{dref} and V_{qref} the expected phase voltage and amplitude were achieved. Phase angle signal is produced from PWM reference frequency with the help of an oscillator. In the designing of the controller, $\boldsymbol{\omega}$ and $\boldsymbol{\theta}$ were extracted by the help of the PLL block and three phase voltages at the island connection point to the grid V_{abc}^{pcc} (pcc, the point of common coupling) are measured. The currents generated by DG are metered and transformed into dp frame (I_d and I_q) using θ, the extracted angle by the PLL.

The paper concluded that the power electronics converters with high reliability, least delay, and high compatibility had been used for the voltage and frequency control of the microgrid in an islanding event for the effectiveness of the designed controller.

P. Chiradeja conducted a study in this paper [23], and it was found out that DG is capable of reducing line loss in a distribution network. The paper considered and modeled two simple radial systems, which are systems with DG and systems without DG. After performing line loss analysis for both systems, the system without the DG has the highest loss compared to the system with DG.

Chapter 3: Design Methodology

3.1 Design Decisions

Table 3.1: Design decision for the system under study and Islanding Detection Method

Design No.	Descriptions and Features
Design 1	100 kW PV array, a DC-DC Boost Converter with MPPT and PI, the three-phase inverter of 10 kHz switching frequency, LCL filter, RLC load, a three-phase circuit breaker of 417A is used for initiating islanding, Utility Grid. A combination of Rate of change of voltage (ROCOV) and a change in output waveform at the inverter in islanding detection. The ROCOV method monitors the change $\frac{dV}{dt}$. Islanding is declared if the change in voltage is not within the $1.1 \leq V_{pu} \leq 8.8$ allowable limits, which is the IEEE Std 1547 stipulated value. The change in three-phase output waveform at the inverter during islanding is used to determine islanding event. A three-phase fault (LLL), grid disturbance is simulated for 1s and the waveform compared to that of islanding event for differentiation and to avoid false tripping of the Upstream CB1 (grid side)
Design 2	500 kW PV array, a single-phase inverter, LC filter, RC load, 30 kVA transformer for isolation. A 2.083kA single-phase circuit breaker is used to initiate the islanding condition. The use of Power Line Communication method (PLC) IdM for islanding detection involves sending a signal from the inverter to Grid to check the status of the circuit breaker and determine the presence of islanding.
Design 3	1 MW microgrid consisting of (Mini hydro, 100 kW PV array, a 30 kVA Genset, three 12 V lead-acid Battery, Slide mode frequency shift (SMFS) detection method is used. A three-phase circuit breaker of 4.17 kA initiates the islanding scenario.
Design 4	45 kW microturbine, Two 12 V lead-acid batteries. A three-phase circuit breaker of 417 A, Sandia voltage shift (SVS) method for detection,

3.2 Pugh Matrix

The Pugh Matrix below is used to assess the various design options, which is based on cost, feasibility, complexity, system degradation, reliability, detection speed, and Non-detection zone (NDZ). The various design options are score base on the system requirements and functionality parameters, and the design with the highest score is chosen to be used as the best design for the project.

Table 3.1: The Pugh matrix for scoring each design against the given weight.

Criteria	**Weight**	**Design 1**	**Design 2**	**Design 3**	**Design4**
Cost	5	1	2	3	4
Feasibility	4	5	-2	-3	3
Complexity	7	2	2	4	2
System degradation	2	3	3	2	-4
Reliability	3	-1	-2	3	3
Detection speed	3	4	1	2	-1
Non-Detection Zone	2	5	4	1	2
Total	26	19	8	12	9

From the Pugh matrix above, design 1 has the highest score. The highest score of 19 shows that design 1 is the best design choice compared to the rest of the designs in terms of the system requirements and functionality of cost, feasibility, complexity, system degradation, reliability, and detection speed.

Chapter 4: Materials and Methods

4.1 Introduction

In this chapter, the overall system understudy for this project is clearly outlined with the various components of the system. The different components of the overall system are discussed and modelled with specifications.

4.2 The System Under Study

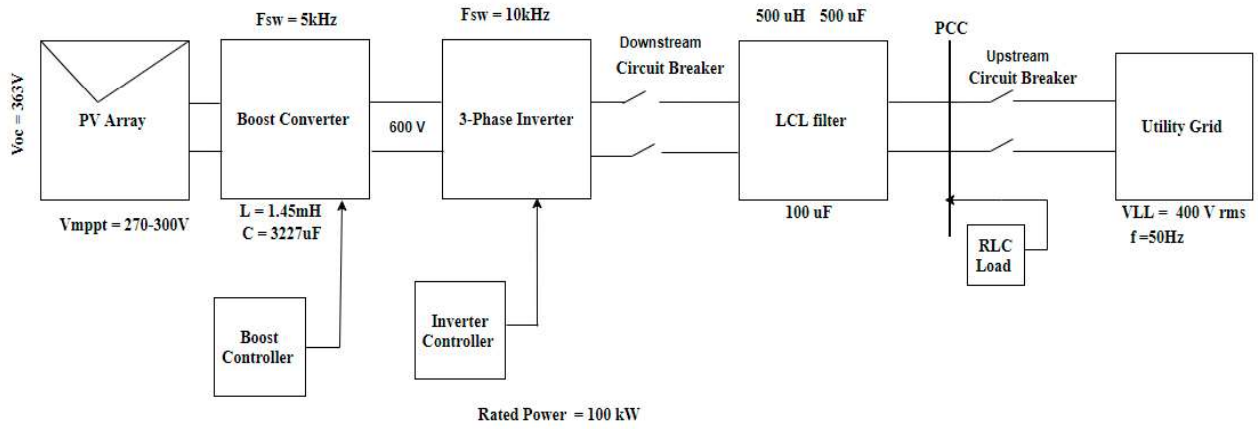

Fig.4.1: 100 kW PV System Under Study

Fig.4.1 shows the complete system understudy for this project. The system has PV panel made of Monocrystalline with an open-circuit voltage of 363V and with maximum power point voltage ranging from 270 V to 300 V. The PV panel is connected to a DC-DC boost converter with a switching frequency of 10kHz, converter inductance of 1.45mH, and converter capacitance of 3227uF. The Boost converter has a boost controller embedded into it to boost the PV panel's output voltage. The output voltage of 600V for the boost converter is connected to a three-phase inverter through a downstream three-phase circuit breaker. The inverter has a switching frequency of 10kHz and with an inverter controller. The output of the three-phase inverter is connected to the utility grid via LCL filter, PCC, and upstream three-phase circuit breaker. LCL filter is

connected at the inverter's output in order to remove harmonics current produced by the inverter. A 3-phase circuit breaker is used to interconnect the DG with the grid. The upstream (grid side) circuit breaker is use for initiating the unintentional islanding. Both the downstream (DG side) and the upstream (grid side) circuit breakers are used for controlling the islanding such that the two breakers are open in order to de-energize the entire system after detecting the islanding and a set voltage threshold has been met.

4.2.1 Design of PV Model

The photovoltaic system used for the project is modelled with the appropriate equations and specifications.

Table 4.1: The specification of the solar panel

Characteristics	**Parameters**
Manufacture	Aria Solar Co
Model name	AS-M60
Cell type	Monocrystalline
Number of cells	48cells
Maximum power rating ($P_{maximum}$)	60 Wp
Open circuit voltage (V_{oc})	28.8 V
Short circuit current (I_{sc})	2.65 A
Maximum power point voltage (V_{mpp})	23 V
Maximum power point current (I_{mpp})	2.16A
Cell open circuit voltage	0.6V
Module efficiency (at STC)	13.7%

Table 4.1: The specifications for the photovoltaic system used for the study and the simulation.

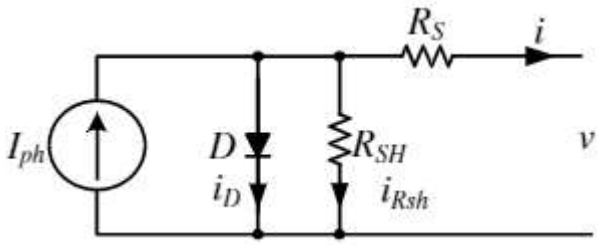

Fig. 4.2: Electrical model of a photocell

$$I = I_{ph} - I_d - R_{sh} \tag{4.1}$$

$$I_{ph} = I_{sc}(\frac{\phi}{1000}) \tag{4.2}$$

$$I_d = I_o\ [\frac{q(V+r_{sI})}{e^{nkT}-1}] \tag{4.3}$$

$$I_{Rsh} = \frac{V+r_{sI}}{R_{sh}} \tag{4.4}$$

From the equivalent equations of I_{ph}, I_d and I_{Rsh} the current of the real model of the photocell is deduced as,

$$I_{ph} = \mathrm{I_{sc}}\left(\frac{\phi}{1000}\right) - I_o\left(\frac{q(V+r_{sI})}{e^{Vt}-1}\right) - \frac{V+r_{sI}}{r_{sh}} \tag{4.5}$$

Given that,

$$V_T = \frac{nkT}{q} \tag{4.6}$$

$\mathrm{I_{ph}}$ = Photocurrent

$\mathrm{I_{sc}}$ = Short circuit current

ϕ = Irradiation (W/m^2)

$\mathrm{I_o}$ = Reverse saturation current (dark current)

q = electron charge, 1.60× $10^{-19}C$

V = Output voltage (V)

k = Boltzmann's constant, 1.38× $10^{-23}\frac{J}{K}$

I_{Rsh} = Current diverted by shunt resistance, I_{Rsh}

$\mathrm{I_d}$ = Current of diode

4.2.2 Boost Converter Design with MPPT Algorithm

To be able to derive the maximum power from the PV panel, Maximum power point algorithm is implemented in the Boost converter. The $Vmppt$, of the PV system, ranges from 270V- 300V. But in order to get 100kW from the system, the designed and desired output voltage must be 600V. Hence, the Boost converter was designed to increase the output voltage of the PV panel from 300V to 600V. To achieve this, Perturb and Observe algorithm is used to implement the MPPT algorithm to derive the maximum power from the PV panel. The P&O algorithm is used as it is easy and simple to implement compared to the other Maximum power point algorithm methods.

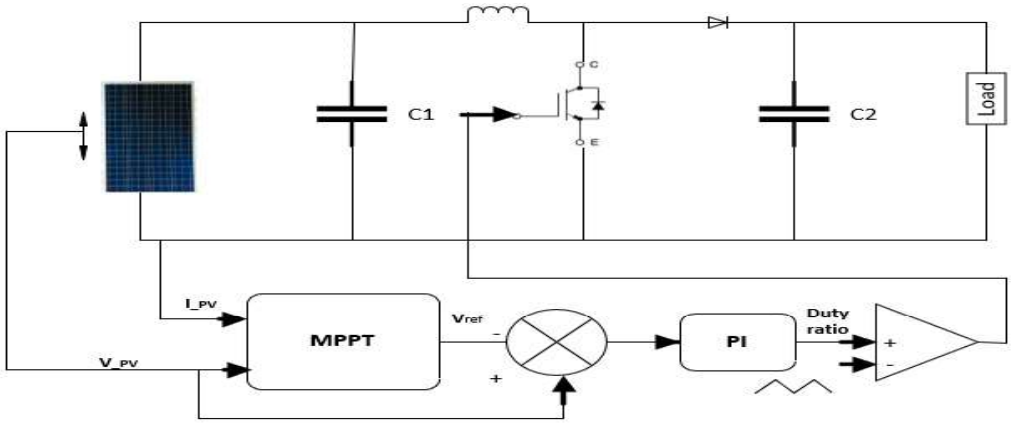

Fig.4.4: Boost Converter with MPPT algorithm using P&O method

Fig.4.4 above is the block diagram which shows the implementation of the Boost converter with MPPT algorithm. From Fig. 4.4, both PV voltage and current are sent to the MPPT controller, and the output of the MPPT controller is the voltage reference which is compared to the actual PV voltage, and the error term is then fed to Proportional and Integral controller. The output of the PI controller gives the required duty ratio for Pulse Width Modulation, which is compared with the carrier signal and the output given to the gate terminal of IGBT switch. This method gives a better MPPT tracking performance since it has a close loop control mechanism. In order to the get the

desired output of the PV system to be 100k W, the following specification of the Boost converter has to be met and hence, the table below gives the values for the design.

Table 4.2: Design Specification of Boost converter

Input Voltage	270-300V
Output Voltage	600V
Rated Power	100kW
Switching frequency, fsw	5kHz
Ripple current, ΔI	5%
Ripple Voltage, ΔV	1%

Table 4.2 above shows the specifications of the boost converter designed for the photovoltaic system. The percentage values are chosen for the ripple current and ripple voltage based on the IEEE Std 1547 and design decisions and choices made in order to achieve the maximum efficiency of the boost converter. The calculations of the design parameters are shown below.

Input Current = $\frac{100kW}{250} = 400A$

Ripple Current = 5% of 400 = 20A

Voltage Ripple = 1% of 600 = 6V

Output Current = $\frac{100kW}{600} = 166A$

Inductance, L = $\frac{V_{ip}(V_{op}-V_{ip})}{f_{sw}*\Delta I*V_{op}} = 1.45mH$ (4.7)

Capacitance, C = $\frac{I_{op}(V_{op}-V_{ip})}{f_{sw}*\Delta V*V_{op}} = 3227uF$ (4.8)

In the DC-DC Boost converter's design, the equation that relates the input to the output voltage and the input and outputs current relationship were derived. Also, a design equation for sizing the

inductor was derived. For the design, it is assumed that the input power is the same as output power, and the current flowing through the inductor is continuous; thus, the converter is in continuous conduction mode. The maximum and the minimum currents through the inductor when the low side switch (IGBT switch) and high side switch (Diode switch) is turn Off and On are given as;

$$I_{mx} = \left(\frac{1}{L}\right) * DT_s + I_{mi} \quad (4.9)$$

$$I_{mi} = \left(\frac{1}{L}\right) * (V_i - V_o) * (1 - D)T_s + I_{mx} \quad (4.10)$$

The input and output voltage relationship across the load is derived from (1) and (2), which is.

$$V_o = \frac{V_i}{1-D} \quad (4.11)$$

Also, the input and output current relation is derived from (1) and (2) on the assumption that input power is the same as output power as;

$$I_i = \frac{I_o}{1-D} \quad (4.12)$$

From the (3) and (4), it can be seen that output voltage increases whiles output current decreases by a factor of (1-D)

Where D is the duty cycle of the low side switch (IGBT switch side)

The inductor sizing is calculated as;

$$L = \frac{(V_i * D)}{f_s * \Delta I_L} \quad (4.13)$$

The IGBT, diode, and capacitor sizing are given as,

$$P_{Qcond} = \left(\frac{I_o}{1-D}\right)^2 R_{DS} D \ , V_{DS} > V_i \quad (4.14)$$

$$P_D = V_o * I_O \ , V_{RRM} = V_o \quad (4.15)$$

$$C = \frac{I_o * D}{f_s * \Delta V_o} \quad (4.16)$$

4.2.3 Three Phase Inverter Design with Controller

A three-phase inverter was designed for converting the input DC voltage of 600V from the Boost converter into AC voltage so that it can be connected to the utility grid. The three-phase inverter was designed as it handles enough power.

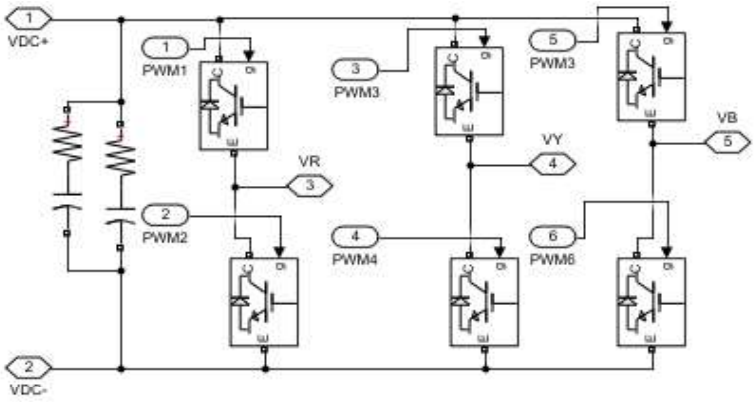

Fig.4.5: Simulink model of a three-phase inverter

The three-phase inverter is made of Six IGBTs switches, and each inverter is controlled with pulse width modulation as it helps modulate the signal angle to get the desired sinusoidal output.

Table 4.3: Specifications for inverter design

Parameters	**Values**
Input Branch Capacitor	1000μF
Resistance	1mΩ
IGBT/Diode	
Internal Resistance (R_{cn})	1mΩ
Snubber Resistance (R_s)	500kΩ
Snubber capacitance (C_s)	1mF

Table 4.3 above gives specifications of the three-phase inverter design for the PV grid connection. The input bus capacitor branch of $1000\mu F$ and resistor of $1m\Omega$ reduces any voltage variations

effects as the irradiance and load vary. The inverter consists of six IGBT/Diode connected in parallel with internal resistance, snubber resistance, and snubber capacitance of $1m\Omega$, $500k\Omega$, and $1mF$, respectively.

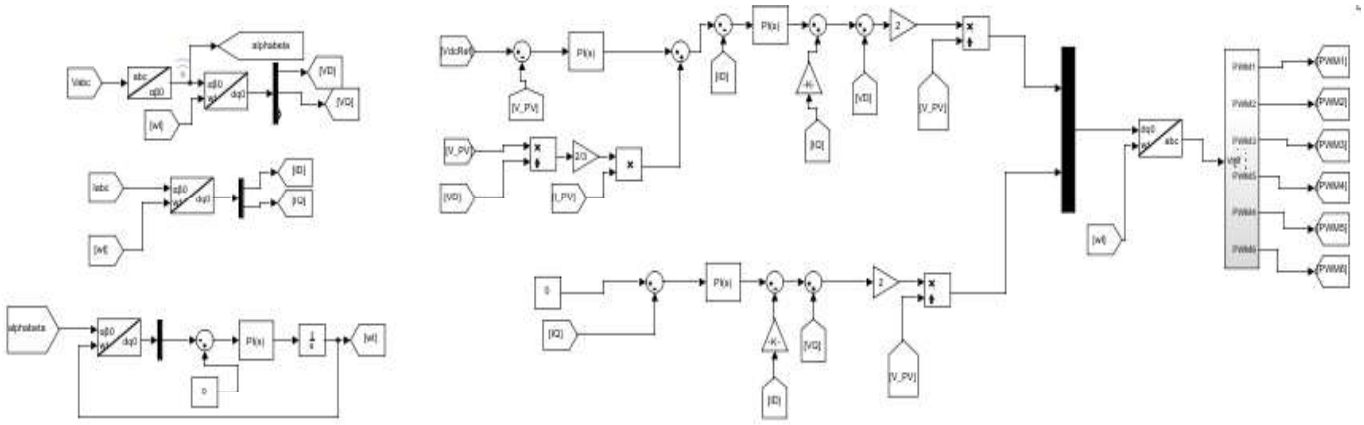

Fig.4.6: Simulink modelled of Boost converter controller and three-phase inverter controller

The above Fig.4.6 is a three-phase inverter controller consisting of three controller components which are voltage and current transformation controllers and Phase-Locked Loop. The design of inverter controller is imperative because it is made of IGBTs which need to be controlled so as to get the desired output. The voltage controller sensed the three-phase line voltages V_{abc} at the grid side and transformed into two-phase alpha, beta voltages V_α, V_β . The transformation was achieved by using Park transformation. The V_α, V_β voltages are then converted into V_d, V_q voltages using Clark transformation. Phase-Locked Loop is implemented using the alpha, beta voltages. The PLL ensures that the inverter output current is synchronized with the grid voltage.

4.2.4 LCL Filter Design

The design of an LCL filter for three-phase grid-connected is crucial as it helps reduce the current harmonics from distorting the AC voltage and current of the utility grid. An LCL filter was

chosen and design for this project as it proves to work better in reducing the harmonics current that might interfere AC waveform of the grid.

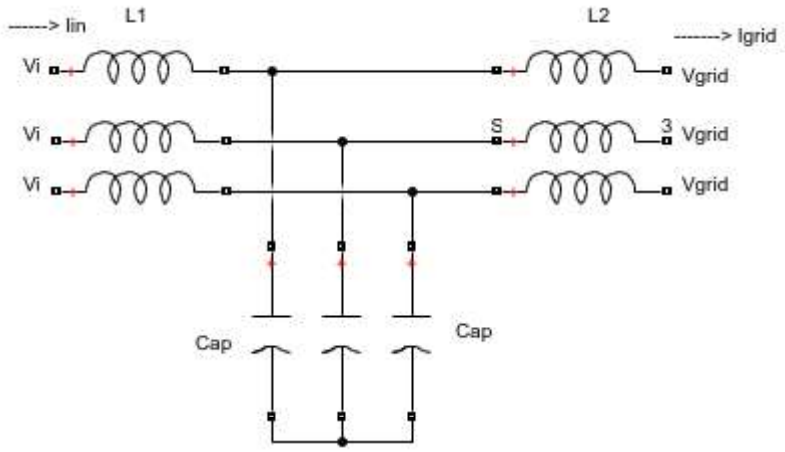

Fig.4.6: LCL filter for three-phase grid-connected inverter

The above Fig 4.6 shows an LCL filter consisting of two inductors and a capacitor. The LCL filter is designed for the inverter's grid side to reduce the current harmonics injected into the grid. The design is done such that the filter follows the IEEE Std.1547 of allowable THD for photovoltaic grid connection, which should not exceed 5%.

The Laplace equation relating the input and output of the inductor is given below

$$\frac{V_i - V_x}{sL1} = I_g + \frac{V_x}{\frac{1}{sC}} \quad (4.17)$$

$$V_X = I_g sL2 \quad (4.18)$$

Where V_i is inverter voltage

I_g is the grid current$LI\ and\ L2$ are inductor 1 and 2, respectively

ω_{res} is the resonant frequency, C and L_p is capacitor and peak inductance, respectively

From (4.1) and (4.2)

$$\frac{I_g}{V_i} = \frac{1}{sL(1+S^2CL_p)} \quad (4.19)$$

$$\omega_{res} = \frac{1}{\sqrt{CL_p}} \quad (4.20)$$

Based on the system constraints, size, cost of components, and thermal consideration, the desired value for switching frequency (F_{sw}) is chosen as 10KHz. The resonant frequency is selected such that it is well separated from the switching frequency and follows the IEEE 1547 standard. It is calculated as $f_{res} = \frac{F_{sw}}{10} = \frac{10k}{10} = 1kHz$. The capacitance value is selected based on the capacitor's reactive power requirement, which is limited to 5% of rated power (S).

The capacitance value is calculated as C = $\frac{0.05*S}{V^2*2*pi*f}$

4.2.5 Islanding Load Modelling

The islanded load is modelled as RLC. The RLC load caters for all load types in power system.

This is a general load that comprised RLC elements under sinusoidal-steady-state excitation.

The load current is of the form.

$I(t) = I_{max} \cos(wt + \beta)$ A (4.21)

Instantaneous power absorbed by the load is given as

$p(t) = v(t)i(t) = V_{max} I_{max} \cos(wt + \delta) \cos(wt + \beta)$ (4.22)

$p(t) = VI_R\{1+\cos[2(wt + \delta)]\} + VI_X \sin[2(wt + \delta)]$ (4.23)

4.2.4 Three Phase Circuit Breaker Sizing

Two 3-phase circuit breakers have been selected and designed for the PV grid connection. The breakers include upstream CB (grid side) and downstream CB (PV side). The sizing of the circuit breaker was done as follows.

The connected load is RLC with a rating of 100kW.

Voltage = 400V, power factor(pf) is 0.8 and

The KW is converted to KVA as.

$$KVA = \frac{KW}{pf} = \frac{100}{0.8} = 125\ KVA$$

$$Current, I = \frac{Connected\ Load}{\sqrt{3}\ * V} = \frac{125 * 1000}{\sqrt{3}\ * 400} = 180.42\ A$$

Where kW = Kilowatt

KVA = Kilovolt ampere

V = voltage

For the desired constraints and requirement, safety factor was assumed to be 25% for the CB;

The required circuit breaker $= Current\ (I) * 25\%\ safety\ factor$

$$= I * 1.25 = 180.42 * 1.25 = 225.53\ A$$

4.2.4 Grid Synchronization Under Normal Conditions

The photovoltaic is synchronized with the grid under normal conditions of frequency, voltage, phase angle. It is imperative to synchronize the grid to know the grid's status by matching the oncoming frequency, voltage, and phase angle of the photovoltaic system and the utility grid.

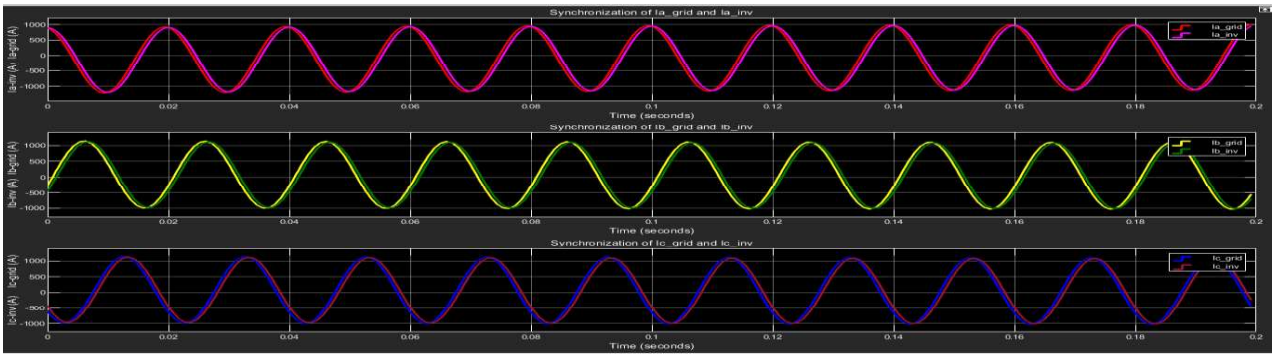

Fig.4.7: Synchronization of three-phase grid current and inverter current

In above Fig 4.7 depicts how the inverter currents and utility grid currents are in synchronism. The synchronization was done for all three phases for the currents. The graphs show that the inverter and the utility grid's three-phase current are matching, and hence maximum power of 100 kW can be transferred from the photovoltaic system to the grid.

4.3 The Proposed Unintentional Islanding Methodologies

The islanding detection methods designed and modeled for these projects are Rate of Change of Voltage (ROCOV) and Harmonic distortion factor. For the ROCOV method, the voltage at the output of the inverter at the point of common coupling (PCC) would be measured before and after islanding event. The measured voltage value would be compared to a standard pre-defined threshold, and if not within the threshold, islanding would be declared.

For the harmonic distortion factor method, the harmonic would be measured for normal grid interconnection and for islanding event, and if the values are above the required IEEE Std 1547 value of 5%, for DG integration, islanding condition would be declared to have occurred.

4.3.1 Design of ROCOV Islanding Detection Method

Rate of change of voltage (ROCOV) or the nature of sine waveform is used as the islanding detection method for this project. For normal grid connection, the inverter current, voltage, power, and frequency are in synchronism with the utility grid. The voltage at the inverter output is measured before and after islanding condition. For unintentional events, the voltage varies with time continuously and significantly, and this voltage is measured, scoped, and compare to the IEEE Std threshold of $1.1 < V_{pu} < 8.8$ or normal voltage sine waveform for grid connection. In the event of islanding, where voltage changes at the point of common coupling (PCC) is not within the threshold of $1.1 < V_{pu} < 8.8$, which is the IEEE Std 1547 acceptable value or the sine waveform is distorted, islanding is then declared to occur.

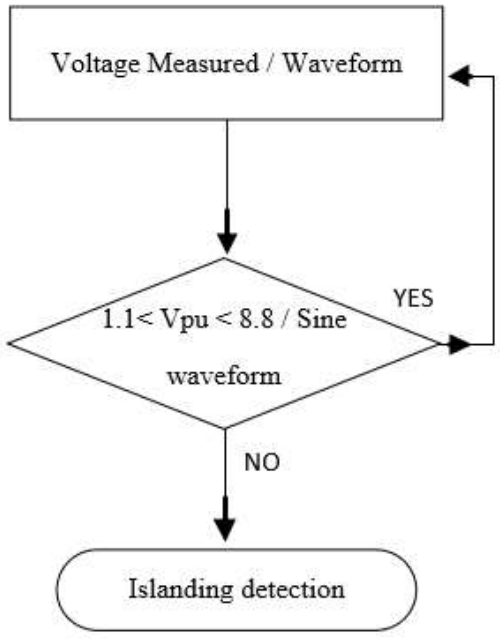

Fig. 4.8: Flow chart of islanding detection based on voltage threshold or voltage sine waveform.

Fig.4.8 above shows the flow chart of the islanding detection based on a set threshold value or normal voltage sine waveform for grid connection.

To able to differentiate islanding event from non-islanding so as to avoid false tripping of the circuit breaker, three-phase fault would be simulated, and its waveform analyzed and compare to islanding event initiated by the opening of the upstream (grid side) circuit breaker.

4.3.2 Design of Harmonic Distortion Islanding Detection Method

The current and voltage harmonic factor is measured at the output of the three-phase grid-connected inverter for both normal grid interconnection and during unintentional islanding conditions. According, to IEEE Standard 1547-2003, for grid interconnection of PV system, the total harmonic distortion of current should not be more than 3%, and that of voltage should also not be more than 5% [24]. And when the measured total harmonic distortion for current, $\mathrm{THD}(_{\mathrm{I}})$ and voltage, $\mathrm{THD}(_{\mathrm{V}})$ are more than 3% and 5% respectively; the grid would have unintentionally islanded from the PV system. Unintentional islanding would be initiated by the opening of the three-phase upstream circuit breaker (grid side).

The equation governing the THD is

$$\mathrm{THD} = \frac{\left(\sqrt{V_n^2 - V_1^2}\right)}{V_1} * 100\%$$

Where,

V_n = n^{th} voltage harmonic factor

V_1 = the fundamental harmonic component

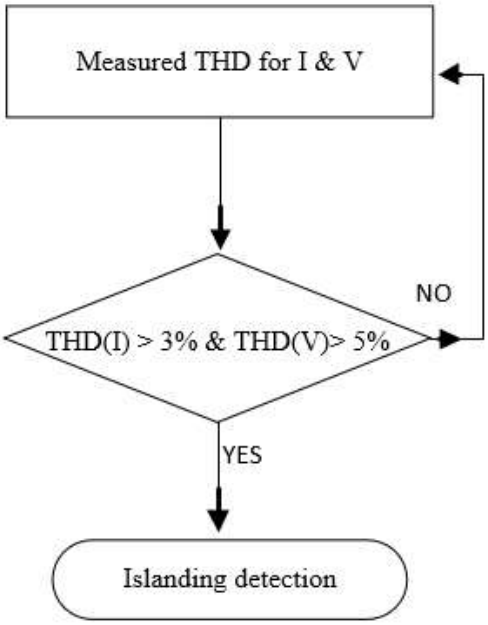

Fig. 4.8: Flow chart of islanding detection based on $THD_{(I)}$ and $THD_{(V)}$

Fig.4.8 above shows the flow chart for the total harmonic distortion of current and voltage method for islanding detection. In order to verify the proper functionality of this method, a three-phase fault would be simulated and compared to the islanding harmonic distortion method.

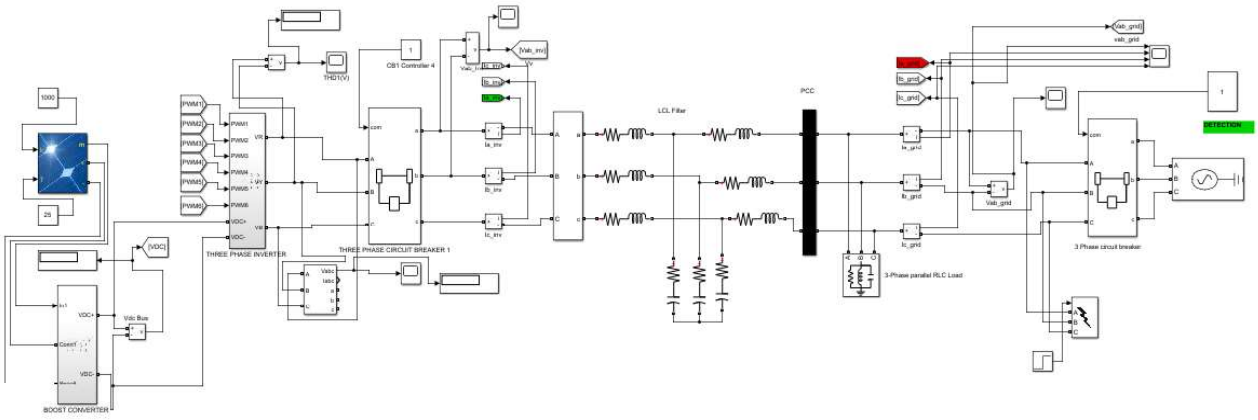

Fig.4.9: Complete Simulink model for the ROCOV and the $THD_{(V)}$ islanding detection methods.

Fig.4.9 shows the complete Simulink model for grid synchronization, islanding detection, and control, three-phase faults. The constant block marker with detection (left green) was used for

initiating the islanding when eternally set to zero as it opens the breaker. The two breakers opened to control the islanding by de-energizing the entire system.

Chapter 5: Results and Analysis

5.1 Introduction

This chapter discusses and analyzes the results obtained in the project. The results for testing the designed system, the various islanding detection methods designed for the project, and the control method would be critically assessed.

5. 2 Result for ROCOV Islanding Detection Method

The design for the ROCOV Islanding detection method has been tested by way of running simulation in MATLAB Simulink for 1second. It was expected that after the utility grid unintentionally islanded from the PV system at PCC, the grid voltage would become zero (non-supplying power). Whiles the PV system still continues supplying power to the RLC load at the PCC. The result of the testing is shown below.

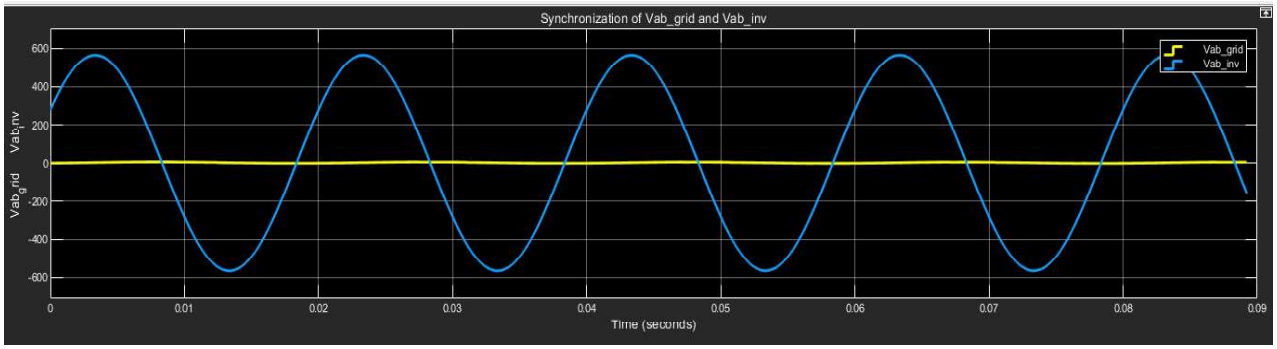

Fig 5.1: The grid and inverter output voltage during islanding

Fig 5.1 above shows the grid voltage (yellow line) and inverter voltage (blue wave) at PCC during islanding detection. It can be seen that the grid voltage was zero when the upstream (grid side) circuit breaker islanded unintentionally. From the graph, it can be seen and analyzed that, even though the upstream circuit breaker has opened, which causes the grid voltage to become zero, the PV system continues to supply voltage to the load it serves at PCC. This shows that

islanding has occurred, and this was detected using rate of change of voltage, $\frac{dv}{dt}$ at the output of the inverter.

5.3.1 Result for Three Phase waveform at PCC in Islanding

The nature of the three-phase waveform between the grid and the inverter at the PCC was another method used for detecting islanding, and it was expected that during islanding, the sinusoidal waveform would be distorted. A Three-phase fault (non-islanding) is simulated and compared with the islanding event (opening of CB1) in order to differentiate between the condition based on the nature of the waveform and avoid false tripping. The results are shown below.

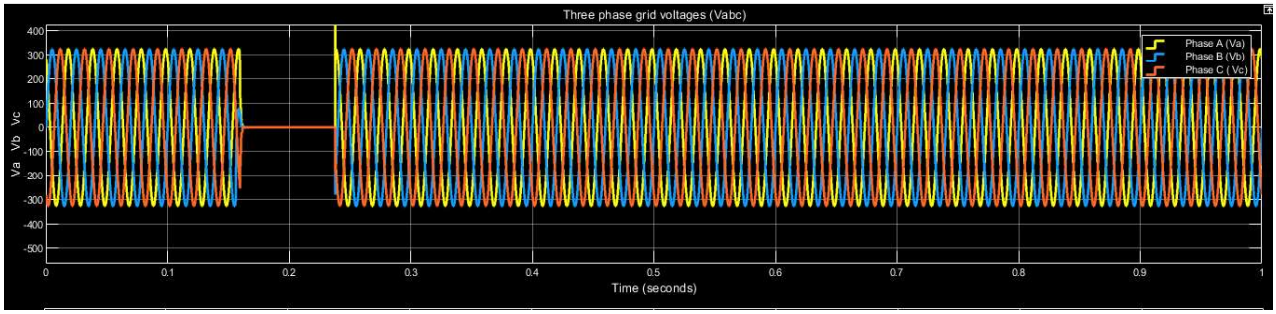

Fig.5.2: Three-phase voltage waveform after islanding condition.

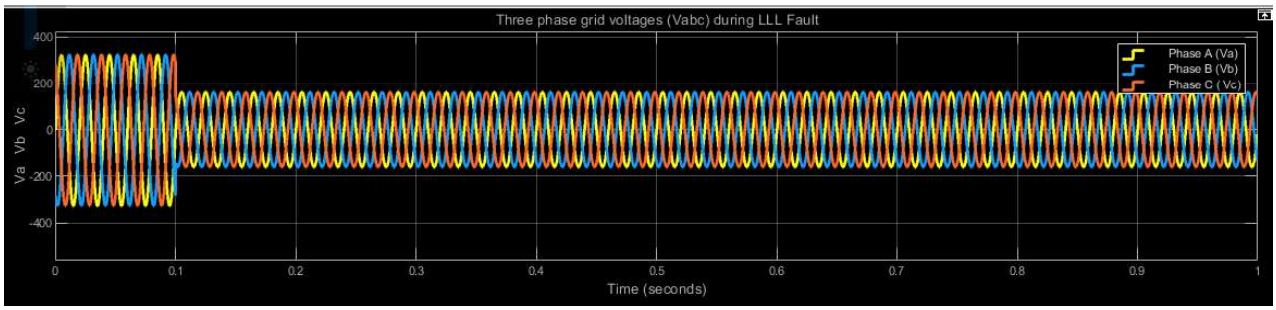

Fig 5.3: Three-phase grid voltage waveform during LLL fault condition.

Fig.5.2: shows the three-phase grid voltage waveform after initiating an unintentional islanding condition at 0.15s and running the Simulink model for 1s. Whiles, Fig.5.3 depicts three-phase grid voltage waveforms in the event of a three-phase fault (LLL), which was initiated at 0.1s using step input function in MATLAB Simulink. Based on these two results, it can be seen and verified that,

the voltage waveforms differ for islanding detection (Fig.5.2) and without islanding detection (Fig.5.3) and using this difference, an islanding condition (opening of circuit breaker) can be differentiated from non-islanding event (grid faults) which avoids false tripping and nuisance.

5.3.2 Results for Harmonic Distortion Islanding Detection Method

Simulation for total harmonic distortion was done in MATLAB Simulink for 1s at a fundamental frequency of 50Hz for five complete cycles. The simulation was done for both normal grid connection and islanding events, and the results are shown below.

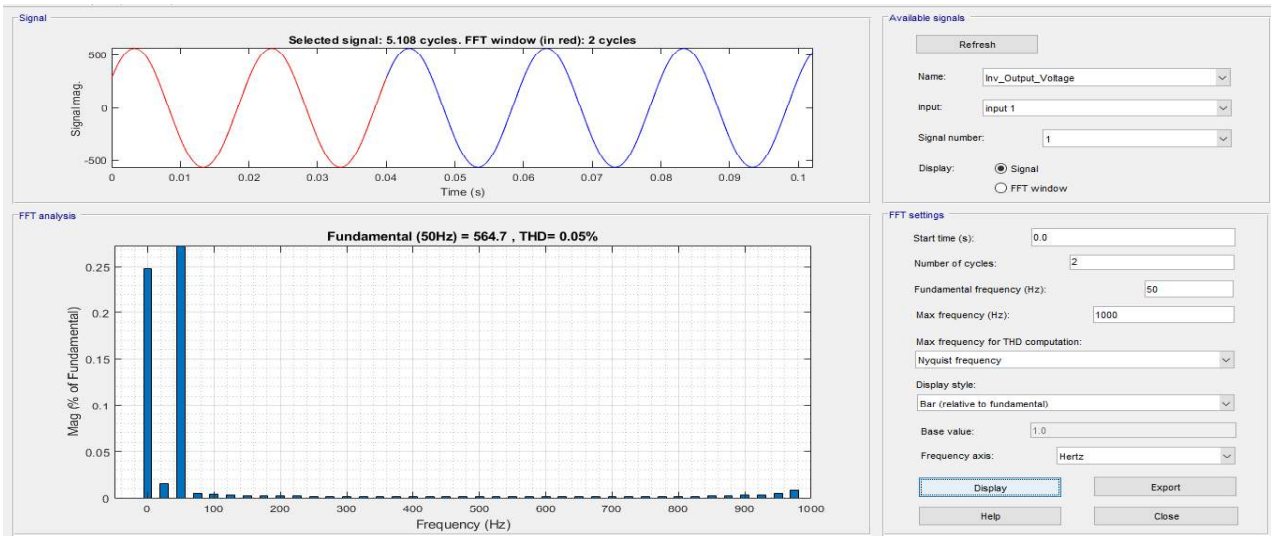

Fig. 5.4: The THD$_{(V)}$ value without islanding detection

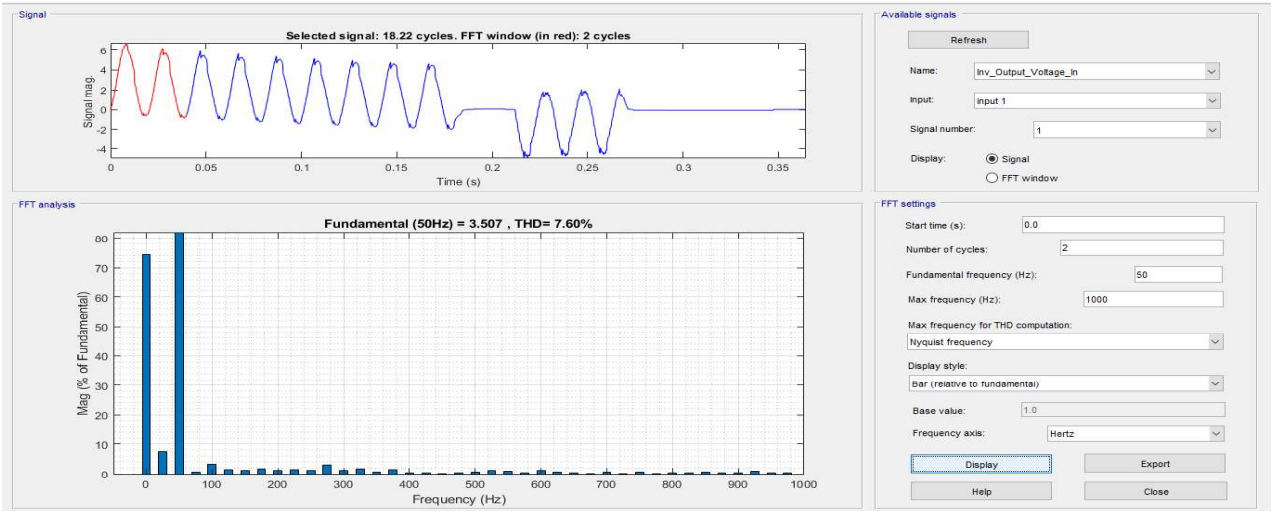

Fig. 5.5: The THD$_{(V)}$ value in islanding mode

Fig.5.4 and Fig. 5.5 above show the total harmonic distortion of voltage without islanding detection and islanding detection event. The total harmonic distortion of voltage was 0.05% without islanding detection. And with islanding detection, it was 7.60%. It can be seen from these results that; the harmonic distortion of voltage was more than seven times that of without islanding detection. The difference between the harmonic distortion for the two scenarios is 7.55%. Unintentional islanding was declared to occur based on this value which is more than 5%, the standard threshold value stipulated by IEEE Std 1547-2003 for normal DG interconnection.

5.5 Result for Unintentional Islanding Detection and Control

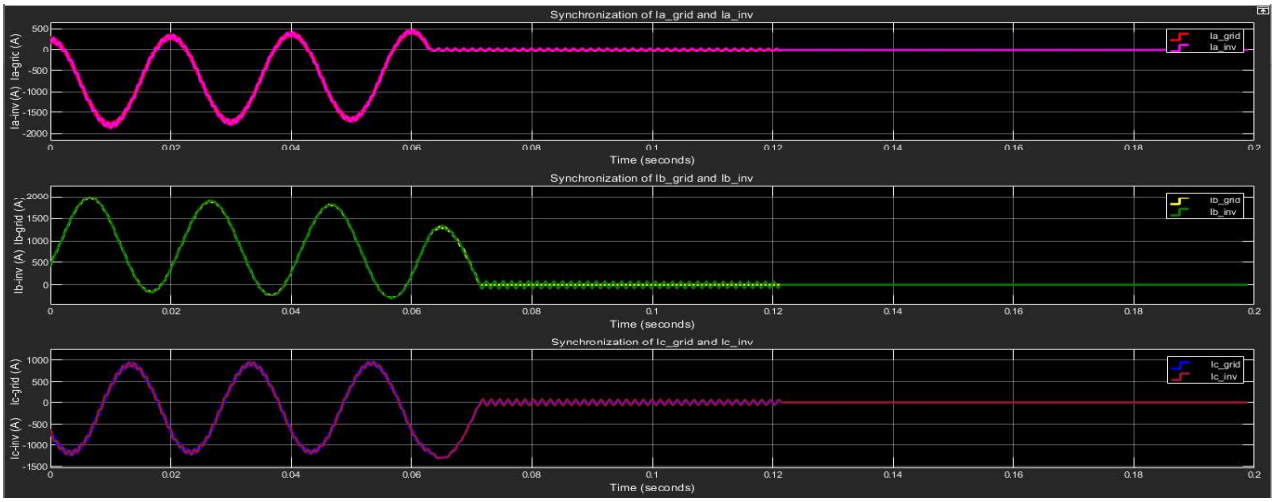

Fig 5.6: Unintentional islanding control by opening both circuit breakers to de-energize the entire system.

Fig.5.6 shows various changes in both the grid and voltage waveform at the output of the three-phase inverter. The graph shows that both the grid and inverter current were in synchronism for the three phases (A, B, and C) for normal grid conditions. This happens from 0s to 0.063s, 0.066s, and 0.066s for phases A, B, and C, respectively. After, this time islanding was detected by opening only the upstream (grid side) circuit breaker, which lasted for 0.12s. During this time, the DG was still supplying current, as can be seen from Fig.5.6. However, both the grid and the inverter current

became zero (no current supplied) after opening both the upstream and downstream circuit breakers, within the time of 0.12s to 0.2s.

The above analysis clearly shows that islanding has successfully been detected and controlled by using the status of the three-phase circuit breakers at the output of the inverter

5.5 Robustness of the LCL filter Designed

The purpose of the LCL filter designed is to eliminate higher harmonic orders for voltage and current from distorting the normal AC waveform for the utility grid, and assessing its performance is crucial to see how best it performs. In determining how best the filter works, the THD for voltage was measured at the output of the inverter, with the filter and without the filter, and both cases were compared. The results for both cases are shown below.

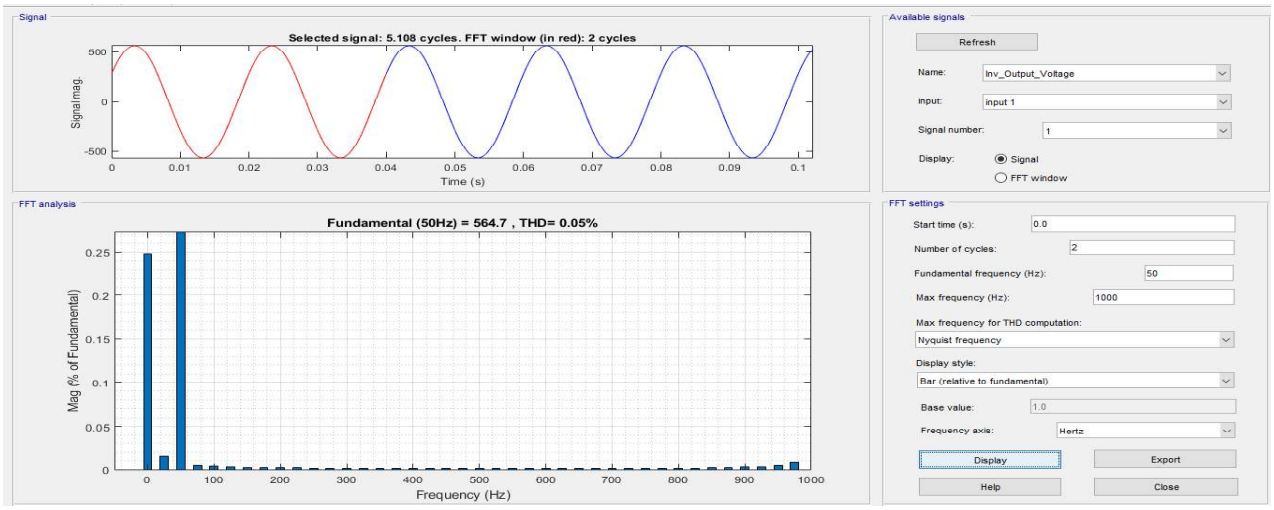

Fig 5.7: Total Harmonic Distortion of voltage, $\mathrm{THD}_{(V)}$ at the inverter output with LCL filter

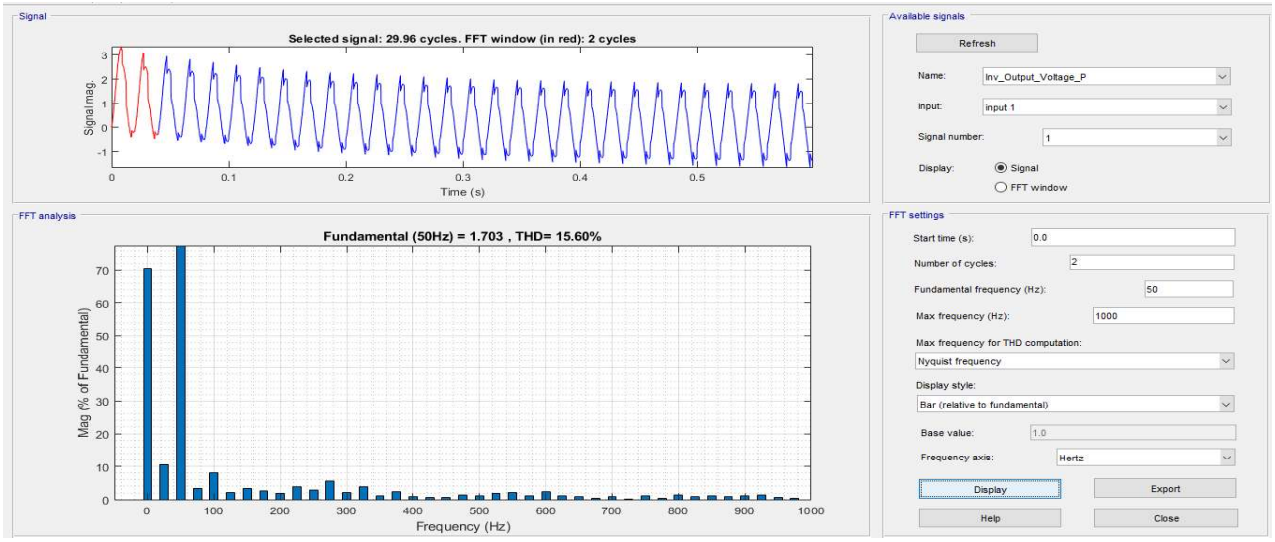

Fig 5.8: Total Harmonic Distortion of voltage, $\mathrm{THD}_{(V)}$ at the inverter output without LCL filter

From Fig.5.7, the total harmonic distortion of voltage with LCL filter was 0.05%, whiles Fig.5.8 shows for a case without the designed LCL filter, and the value was 15.60%, as shown in the graphs above.

The measured $\mathrm{THD}_{(V)}$ value of 15.60% shows the level of distortion of a voltage that might distort the AC waveform of the utility grid. The value measured was more than the 5% $\mathrm{THD}_{(V)}$ which is the required value by IEEE Std 1547-2003. And it can be seen that the LCL filter was able to drastically reduce the level of voltage distortion from 15.60% to 0.05%, which is even better than the IEEE standard $\mathrm{THD}_{(V)}$ for voltage value of 5% for PV interconnection to the utility grid.

Chapter 6: Conclusion and Recommendation

6.1 Introduction

For any projects that have been done, it is imperative to discuss the challenges, successes, limitations, relevant lessons learned, and the necessary recommendations for future projects as it helps to know the outcome of the research and the way forward. This chapter discusses the limitations, future work, lessons learned, conclusion, and recommendation for the project undertaken.

6.2 Limitations

The design, modelling, and MATLAB Simulink implementation work well. Most of the project objectives were achieved. However, some of the objectives, such as the control of the islanding detection, did not function as expected. The control was manually done instead of being automatic.

The project was not implemented on a live distribution system, and there might be small variations during the actual implementation on a live system, as certain assumptions were made during the design process. Also, the project only considers inverter-based distribution generations and cannot be replicated for multiple DG systems.

6.3 Future Work

The projects seek to design and modelled islanding detection in distributed generations. 100 kW photovoltaic system was designed and modelled as the system under study; thus, only inverter-based DG was considered in this paper.

Future projects should look at multiple DG systems, such as combining a mini-hydro, reciprocating engine, micro wind turbine. Also, this project only used passive islanding detection method, and future projects should consider active islanding detection. Automatic transfer of power suppliers should be design and implemented as an effective unintentional islanding control strategy. Also, Future studies should also look at implementing the design on a live distribution network.

6.4 Conclusion and Lessons Learnt

This project delved into the design, modelling of islanding detection in distributed generations. A 100kW photovoltaic system has been designed and modelled as the DG for the project work. Like any other project, this project also came far with its own challenges, which brought about certain unique lessons that must be learnt as an upcoming electrical and electronics engineer. PSCAD software was explored and learnt during the projects even though it was not used for the design and the modelling due to certain components not been present in it. MATLAB skills have been well enhanced as it was used entirely for the design and the modelling. Proper and effective researching skills have been improved through series of meticulous analyses of research papers. Also, good experiment structuring and data analyzing skills have been improved by going through series of iterations of design and experimentations.

In conclusion, the use of ROCOV, Total harmonic distortion, and change in sine waveform passive islanding detection methods have been successfully implemented using MATLAB Simulink simulation. The use of change in sine waveform method for islanding detection was able to differentiate islanding event (opening of downstream CB) and non-islanding condition such as three-phase fault. Islanding detection time was 0.15s, and this value is within the IEEE Std 1547 allowable limit of 2s for DG disconnection during an islanding event. The use of the passive islanding detection method would be able to save implementation costs. The design, modeling, and

implementation of a 100kW photovoltaic grid-connected system have been successful. This project can be used for further research, and it can be implemented on a live distribution network.

References

[1] P. Mahat, Z. Chen, and B. Bak-Jensen, "Review of islanding detection methods for distributed generation," *3rd Int. Conf. Deregul. Restruct. Power Technol. DRPT 2008*, no. April, pp. 2743–2748, 2008, doi: 10.1109/DRPT.2008.4523877.

[2] F. Gonzalez-Longatt and C. Fortoul, "Review of the distributed generation concept: Attempt of unification," *Renew. Energy Power Qual. J.*, vol. 1, no. 3, pp. 281–284, 2005, doi: 10.24084/repqj03.275.

[3] N. Acharya, P. Mahat, and N. Mithulananthan, "An analytical approach for DG allocation in primary distribution network," *Int. J. Electr. Power Energy Syst.*, vol. 28, no. 10, pp. 669–678, 2006, doi: 10.1016/j.ijepes.2006.02.013.

[4] S. Conti, "Analysis of distribution network protection issues in presence of dispersed generation," *Electr. Power Syst. Res.*, vol. 79, no. 1, pp. 49–56, 2009, doi: 10.1016/j.epsr.2008.05.002.

[5] A. Shrestha *et al.*, "Comparative Study of Different Approaches for Islanding Detection of Distributed Generation Systems," *Appl. Syst. Innov.*, vol. 2, no. 3, p. 25, 2019, doi: 10.3390/asi2030025.

[6] F. Noor, R. Arumugam, and Y. Mohammad Vaziri, "Unintentional islanding and comparison of prevention techniques," *Proc. 37th Annu. North Am. Power Symp. 2005*, vol. 2005, pp. 90–96, 2005, doi: 10.1109/NAPS.2005.1560507.

[7] M. S. Kim, R. Haider, G. J. Cho, C. H. Kim, C. Y. Won, and J. S. Chai, "Comprehensive review of islanding detection methods for distributed generation systems," *Energies*, vol. 12, no. 5, pp. 1–21, 2019, doi: 10.3390/en12050837.

[8] IEEE Standards Coordinating Committee 21 on Fuel Cells Photovoltaics Dispersed Generation and Energy Storage, *IEEE Recommended Practice for Utility Interface of Photovoltaic (PV) Systems*, vol. 2000. 2000.

[9] T. Basso and N. Friedman, "IEEE 1547 National Standard for Interconnecting Distributed Generation : How Could It Help My Facility ?," *http://www.osti.gov/bridge Available*, no. November, p. 9, 2003, [Online]. Available: http://www.nrel.gov/docs/fy04osti/34875.pdf.

[10] Ministry of Energy, Energy Commission, Ministry of Science and Technology of China, and UNDP, "Ghana Renewable Energy Master Plan," *Ghana Renew. Energy Master Plan*, pp. 1–83, 2019.

[11] H. Karimi, A. Yazdani, and R. Iravani, "Negative-sequence current injection for fast islanding detection of a distributed resource unit," *IEEE Trans. Power Electron.*, vol. 23, no. 1, pp. 298–307, 2008, doi: 10.1109/TPEL.2007.911774.

[12] C. Li, C. Cao, Y. Cao, Y. Kuang, L. Zeng, and B. Fang, "A review of islanding detection

methods for microgrid," *Renew. Sustain. Energy Rev.*, vol. 35, pp. 211–220, 2014, doi: 10.1016/j.rser.2014.04.026.

[13] W. Bower, "Implementing Agreement on Photovoltaic Power Systems Grid Interconnection of Building Integrated EVALUATION OF ISLANDING DETECTION METHODS FOR PHOTOVOLTAIC UTILITY- INTERACTIVE POWER SYSTEMS," 2002.

[14] M. R. Alam, M. T. A. Begum, and K. M. Muttaqi, "Assessing the Performance of ROCOF Relay for Anti-Islanding Protection of Distributed Generation under Subcritical Region of Power Imbalance," *IEEE Trans. Ind. Appl.*, vol. 55, no. 5, pp. 5395–5405, 2019, doi: 10.1109/TIA.2019.2927667.

[15] A. Singh, R. S. Bhatia, S. Chanana, and P. Gupta, "A Passive Islanding Detection Technique for Grid-Connected Photovoltaic Inverters," *2018 IEEE Int. Students' Conf. Electr. Electron. Comput. Sci. SCEECS 2018*, 2018, doi: 10.1109/SCEECS.2018.8546918.

[16] Hans De Keulenaer, "Voltage and Frequency Control of the Grid," *28/11/2007*, no. 2, 2007, [Online]. Available: http://www.leonardo-energy.org/tools-and-tutorials/voltage-and-frequency-control-grid.

[17] M. Reza Ebrahimi, M. Naser Hashemnia, M. Ehsan, and A. Abbaszadeh, "A Novel Approach to Control the Frequency and Voltage of Microgrids in Islanding Operation," *Int. J. Eng. Technol.*, vol. 4, no. 5, pp. 562–566, 2012, doi: 10.7763/ijet.2012.v4.433.

[18] D. Reigosa, F. Briz, C. B. Charro, P. Garcia, and J. M. Guerrero, "Active islanding detection using high-frequency signal injection," *IEEE Trans. Ind. Appl.*, vol. 48, no. 5, pp. 1588–1597, 2012, doi: 10.1109/TIA.2012.2209190.

[19] D. Voglitsis, F. Valsamas, N. Rigogiannis, and N. Papanikolaou, "On the injection of sub/inter-harmonic current components for active anti-islanding purposes," *Energies*, vol. 11, no. 9, 2018, doi: 10.3390/en11092183.

[20] A. Timbus, A. Oudalov, and C. N. M. Ho, "Islanding detection in smart grids," *2010 IEEE Energy Convers. Congr. Expo. ECCE 2010 - Proc.*, pp. 3631–3637, 2010, doi: 10.1109/ECCE.2010.5618306.

[21] C. Srinivas, "Control of Grid-Connected and Intentional Islanding Operations of Photo Voltaic System," vol. 44, no. 3, pp. 691–697, 2013.

[22] H. Akagi, Y. Kanazawa, and A. Nabae, "Instantaneous Reactive Power Compensators Comprising Switching Devices without Energy Storage Components," *IEEE Trans. Ind. Appl.*, vol. IA-20, no. 3, pp. 625–630, 1984, doi: 10.1109/TIA.1984.4504460.

[23] P. Chiradeja, "Benefit of distributed generation: A line loss reduction analysis," *Proc. IEEE Power Eng. Soc. Transm. Distrib. Conf.*, vol. 2005, pp. 1–5, 2005, doi: 10.1109/TDC.2005.1546964.

[24] N. Prabaharan and K. Palanisamy, “A comprehensive review on reduced switch multilevel inverter topologies, modulation techniques and applications,” *Renew. Sustain. Energy Rev.*, vol. 76, no. April, pp. 1248–1282, 2017, doi: 10.1016/j.rser.2017.03.121.

Appendix A

MATLAB Code for Maximum Power Point Tracking (MPPT)

```
function Vref = RefGen(V,I)

Vrefmax = 363;
Vrefmin = 0.0;
Vrefinit = 300;
deltaVref = 1;
persistent Vold Pold Vrefold;

dataType = 'double';

if isempty(Vold)
    Vold =0;
    Pold = 0;
    Vrefold=Vrefinit;
end

P= V*I;
dV = V - Vold;
dP = P - Pold;

if dP ~= 0
    if dP < 0
        if dV < 0
            Vref = Vrefold + deltaVref;
        else
            Vref = Vrefold - deltaVref;

        end
    else
        if dV < 0
            Vref = Vrefold - deltaVref;
        else
            Vref = Vrefold + deltaVref;
        end
    end

else Vref = Vrefold;
end

if Vref >= Vrefmax | Vref <= Vrefmin
    Vref = Vrefold;
end
Vrefold = Vref;
Vold = V;
Pold = P;
```

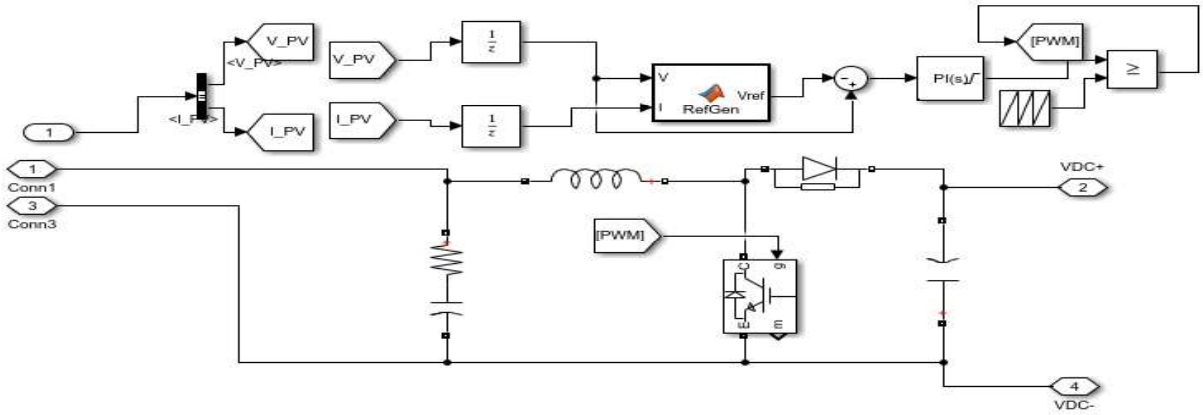

Fig.6.1: DC-DC Boost Converter with MPPT Algorithm using P&O

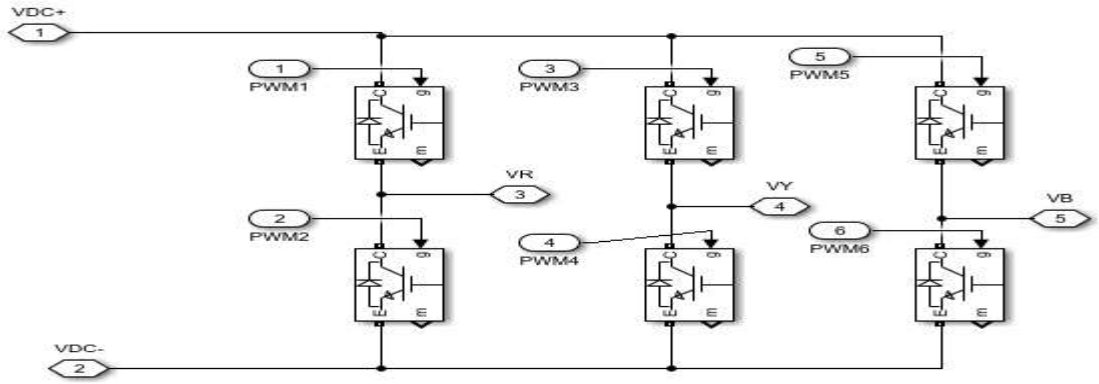

Fig.6.2: Three-Phase Inverter designed

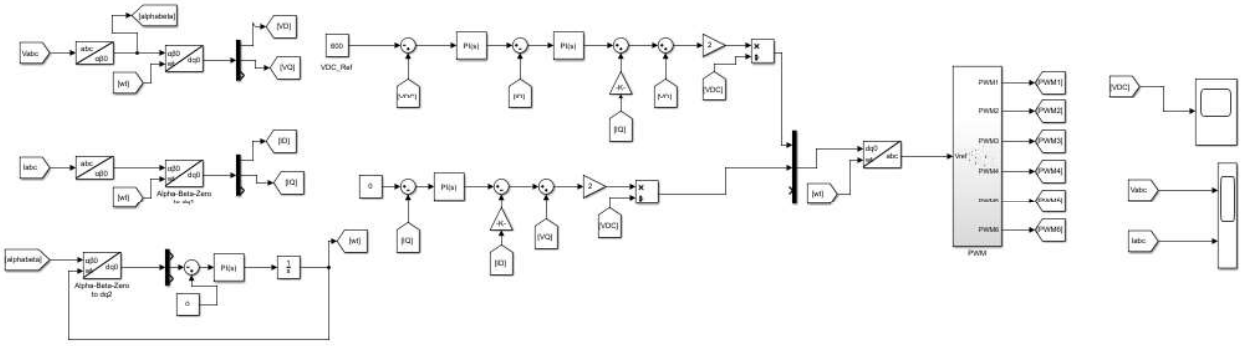

Fig.6.3: DC-DC Boost Converter and Three Phase Inverter Controllers

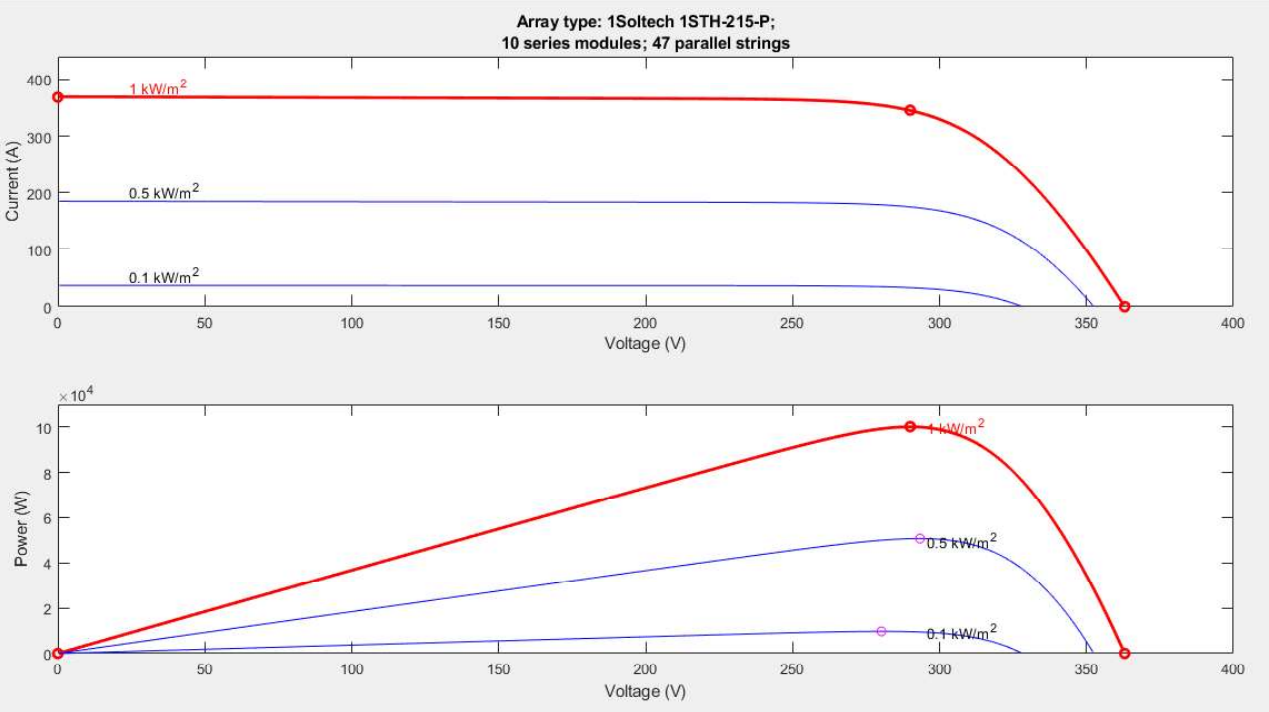

Fig.6.4: Output waveform for PV showing V_{oc}, V_{mpp}, I_{sc} at different radiation.